Int. J. Heat Mass Transfer. Vol. 24, No. 9, pp. 1475 1492, 1981.
Printed in Great Britain

0017 9310/81/091475 18 $02.00/0
Pergamon Press Ltd.

GROWTH OF DIFFUSION-CONTROLLED VAPOUR BUBBLES AT A WALL IN A KNOWN TEMPERATURE GRADIENT

M. G. COOPER
Department of Engineering Science, Oxford University, Oxford, U.K.

and

T. T. CHANDRATILLEKE
Department of Mechanical Engineering, Singapore University, Singapore*

(*Received* 29 *October* 1980 *and in revised form* 16 *March* 1981)

Abstract—Previous studies of individual vapour bubbles growing at a wall into initially stagnant liquid have been extended by introducing controlled initial temperature profiles in the liquid. The simplest such cases were studied first (zero gravity, bulk liquid at saturation temperature), using dimensional analysis and comparing with previous experiments and analysis in an even simpler situation, i.e. initially uniform temperature. Various patterns of behaviour can be seen, which are largely in accordance with expectation, but can now be quantified.

In the absence of gravity, bubbles depart from the wall at times and sizes which can be predicted, at least for bubbles within our range of experimental conditions. That range was extended as far as possible, and corresponds broadly to nucleate boiling at atmospheric pressure or below. For saturation boiling (i.e. $T_{bulk} = T_{sat}$), one particularly simple and universal result is a relation between time and diameter (or volume) at departure. The relation is independent of growth rate and of thermal boundary layer thickness, as it is simply

$$\frac{D_D}{t_D^{2/3}} \simeq 1.5\left(\frac{\sigma}{\rho}\right)^{1/3} \quad \text{or} \quad \frac{V_D}{t_D^2} \simeq 2.0\frac{\sigma}{\rho}.$$

Since σ/ρ does not vary very greatly for normal fluids, this relation is only weakly dependent on the fluid.

The well-established phenomenon of bubbles departing 'against gravity' (i.e. in negative or non-buoyant gravity, as from a downward-facing surface), is now observed for the first time under controlled conditions, and the conditions which favour such behaviour have been identified. These are principally thin thermal boundary layer and strong subcooling.

One unexpected finding is that positive (buoyant) gravity can, in some cases, cause a bubble to depart with larger size than if gravity were absent.

NOMENCLATURE

a, b, c,	constants in equation (3);
$C_1, C_2, \ldots$,	capacitances;
c_p,	specific heat capacity of liquid;
D,	overall width of bubble;
D_D,	value of D at departure;
g,	gravitational acceleration;
g^+,	$g\,Ja^8\alpha^4\,(\rho/\sigma)^3$;
h_{fg},	specific enthalpy change of vaporization;
H,	overall height of bubble;
k,	thermal conductivity of liquid;
K,	constant in Appendix;
L_M,	characteristic length for menisci, $\sqrt{[\sigma/(\rho g)]}$;
Ja,	Jakob number $\rho\,c_p(T-T_{sat})/(\rho_g h_{fg})$;
Ja_b, Ja_w,	Ja with $T = T_b$, T_w, respectively;
Pr,	Prandtl number $\mu\,c_p/k$ for liquid;
R,	radius of bubble;
R_h,	electrical resistance of heater;
t,	time;
t^+,	$t/[Ja^6\alpha^3\,(\rho/\sigma)^2]$;
t_D,	time at departure;
$t_1, t_2, \ldots$,	times in Fig. 4;
T,	temperature;
T_0,	initial temperature;
T_b,	bulk liquid temperature;
T_{sat},	saturation temperature;
$V_1, V_2, \ldots$,	voltages;
V_D,	volume at departure.

Greek symbols

α,	thermal diffusivity of liquid;
δ_s,	thickness of thermal boundary layer (defined in Fig. 8);
ρ,	density of liquid;
ρ_g,	density of vapour;
σ,	surface tension;
τ,	time constant;
μ,	viscosity of liquid;
ω,	subcooling parameter $(T_w-T_b)/(T_w-T_{sat})$;
δ_s^+,	$\delta_s/(Ja^4\alpha^2\,\rho/\sigma)$.

* Previous address: Trinity College, Cambridge University, Cambridge, U.K.

INTRODUCTION

MUCH EXPERIMENTAL and theoretical work has been reported on the behaviour of vapour bubbles, aimed at contributing a physical basis for understanding the complex phenomenon of boiling. To be useful in actual boiling the work must of course allow for the actual physical conditions of boiling, which are generally complicated by the presence of gravity and of other bubbles. But theoretical analyses of bubbles are generally feasible only if they refer to simple conditions. Hence there is a large gap between the theory and actual boiling. Experimental work can bridge that gap, but experiments also become difficult to interpret if they include many of the complications of actual boiling.

In recent years we have carried out a series of tests, firstly with bubbles in environments so simple that some theoretical arguments should be available, and then adding complications in sequence. The first major study in this series was described in [1] and involved producing bubbles at a plane wall in an initially stagnant isothermal liquid in zero gravity. That proved to be readily comprehensible, so gravity (normal to the wall) was restored and it was possible to understand that slightly more complex situation in the light of the understanding of the simpler one.

This paper describes one continuation of that study, involving production of bubbles in an environment closer to that of actual boiling. In the experiments to be described, bubbles were grown into a liquid in a jacketed test vessel (Fig. 1). The liquid was initially stagnant but not isothermal. A known temperature field was set up in the liquid just before growing the bubble, broadly comparable to the fields with thermal boundary layers observed by several experimenters [2–5] when actual boiling occurs at a heated wall.

DESIGN OF EXPERIMENT

It was recognized that the introduction of a temperature field could involve the simultaneous introduction of several new variables into the experimental conditions, and could thus produce several simultaneous trends in behaviour which might be difficult to understand. In previous tests, which used initially isothermal liquid, there was one significant driving temperature difference ($T_0 - T_{sat}$), where T_0 was the initial temperature and T_{sat} the saturation temperature at the prevailing pressure. In order that the first tests described here should introduce the minimum of additional complexity, it was decided that they should be performed with bulk temperature T_b equal to T_{sat} (i.e. saturation boiling), while wall temperature T_w took the place of T_0. Hence there would again be only one significant driving temperature difference, ($T_w - T_{sat}$). The new experiments do, however, contain additional factors due to the shape and thickness of the thermal boundary layer. But that driving temperature difference was imposed suddenly by raising wall temperature from bulk temperature T_b to the chosen T_w for a time t_h (heating time) before growing the bubble. Hence the thermal boundary layer was always of the same shape, the error function ($T_w - T_b$) erf $\{x/[2\sqrt{(\alpha t)}]\}$, so the additional information describing shape and thickness were described by a single parameter which characterised the thickness of the thermal boundary layer. Thus only one additional

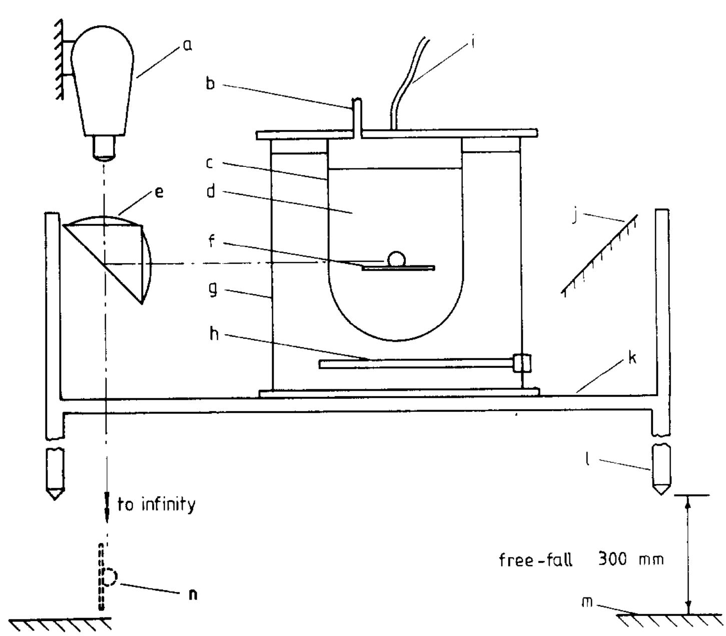

FIG. 1. Sketch of apparatus. a, camera; b, pressure tapping; c, glass bell jar; d, test liquid; e, prism and lens; f, glass heater plate; g, outer jacket; h, bulk liquid heaters; i, electrical connections; j, mirror; k, drop table; l, leg; m, gravel in arrestor bucket; n, bubble image at infinity.

parameter was introduced at that stage. In later tests, further parameters were introduced, by restoring gravity and by making the bulk temperature T_b different from T_{sat}, generally $T_b < T_{sat}$, i.e. subcooled boiling.

Transient heating of wall

For the experiments reported here, we required a heater and associated time-varying power supply to produce a thermal boundary layer of the chosen shape. The heater took the form of a thin layer of electrically conducting material, typically 10 μm of nichrome, some 30 mm square, on the surface of a glass plate. The thickness of the glass exceeded the thermal diffusion distance $[\sqrt{(\alpha t)}]$ for the relevant time, hence it could be regarded as semi-infinite. In order to cause and maintain a step change in temperature at the interface between two semi-infinite bodies (here the glass and the liquid), heat must be supplied at the rate to 'feed' the error function temperature fields developing in each body, i.e. at a rate proportional to $1/(\text{time})^{1/2}$. That clearly has a singularity at time zero, so it could not be followed correctly during some short initial period, t_1, usually a few milliseconds. After that time it would be feasible to supply heat at the required decreasing rate, provided a method could be found for controlling that rate. One method would be to have means of sensing the temperature of the heater and a control loop to maintain that temperature constant. It was realized that a fairly powerful amplifier supplying up to 10 A, 1 kW, would be needed; that can be done, but might introduce problems with ripple from mains supply. A simpler method was adopted, namely to supply the necessary short burst of power from a bank of capacitors, pre-programmed to suit the requirement of power proportional to $1/(\text{time})^{1/2}$. Since the resistance R_h of the heater would not vary greatly, this is equivalent to voltage proportional to $1/(\text{time})^{1/4}$. A single capacitor C_1 would of course produce voltage proportional to $e^{-t/\tau}$ where the time constant τ would be R_hC_1 and, by suitable choice of C_1 and initial voltage, that exponential could match the required curve for a limited time, as shown in line 1 in Fig. 2. The exponential would in due course fall too low, but a second exponential could then be followed if a second capacitor C_2, initially charged to a suitable voltage V_2, was then switched in parallel with C_1 at a suitable time t_2 (after which they discharged together), as shown in Fig. 3(a) and line 2 on Fig. 2. The timing of that switching operation would be crucial, but that problem was readily solved by using a diode instead of a switch as shown in Fig. 3(b). It was then only necessary to charge C_1 and C_2 (and later stages C_3, ...) to appropriate initial voltages V_1 and V_2 (V_3, ...), then on closing the switch H the capacitors discharged in sequence. The actual voltage followed the series of straight lines on Fig. 2 (rounded slightly by diode characteristics) following the required voltage–time curve with accuracy dependent upon the number of stages. Analysis in [6] showed that, by having successive steps at times $t_1, t_2 \ldots$ where $t_n = 2 \times t_{n-1}$, the accuracy was within $\pm 1\%$. For the initial step (which included the signularity) a maximum capacitor voltage of about 100 V was chosen on grounds of safety. That imposed a combined limit on the extent of the temperature step and the time t_1 during which the voltage supply could not be correct. Typically, for a step of 20 K, t_1 was just below 1 ms, but experiments nearly always involved heating times exceeding 20 ms, and in any case the initial step was started early in order to arrange that the integrated energy input [along AB on Fig. 4(a)] was equal to that required [along aB on Fig. 4(a)].

The performance of the complete system of heater and capacitor bank could be monitored by observing the temperature of the heater using thin film resistance thermometers. These were less than 0.5 μm thick, deposited above the heater, and separated from it only by some 4 μm of silicon oxide which gave electrical insulation and close thermal contact [Fig. 5(a)]. A

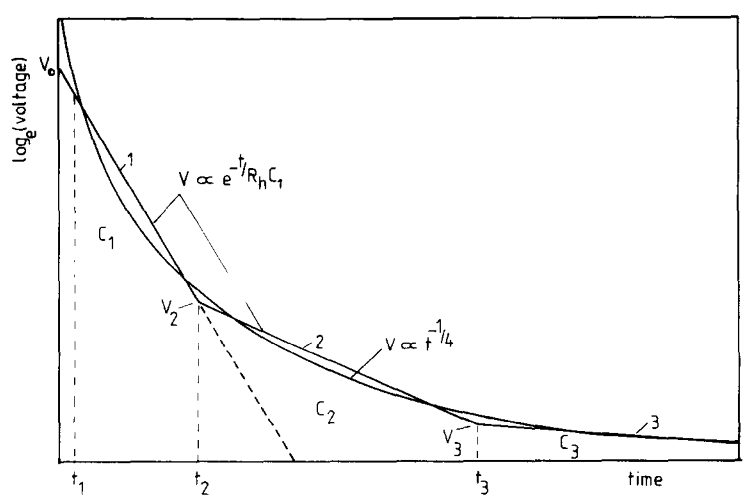

FIG. 2. Voltage–time relationships for heater.

typical result is given in Fig. 4(b), showing a close approximation to a step change and, of course, no problem from mains ripple.

The temperature field caused variations of density in the liquid, and these might cause natural convection. Observations and comparison with theoretical ana-

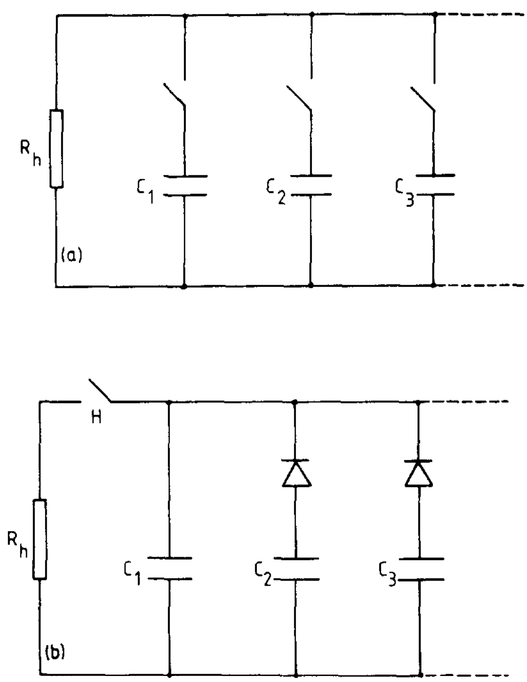

FIG. 3. Capacitor bank supplying electrical heater.

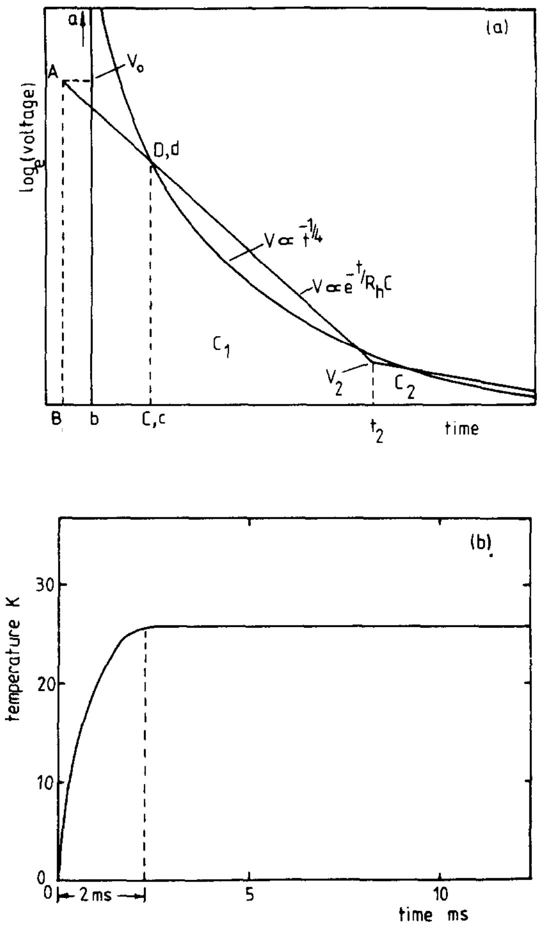

FIG. 4. Power supply and temperature at heater.

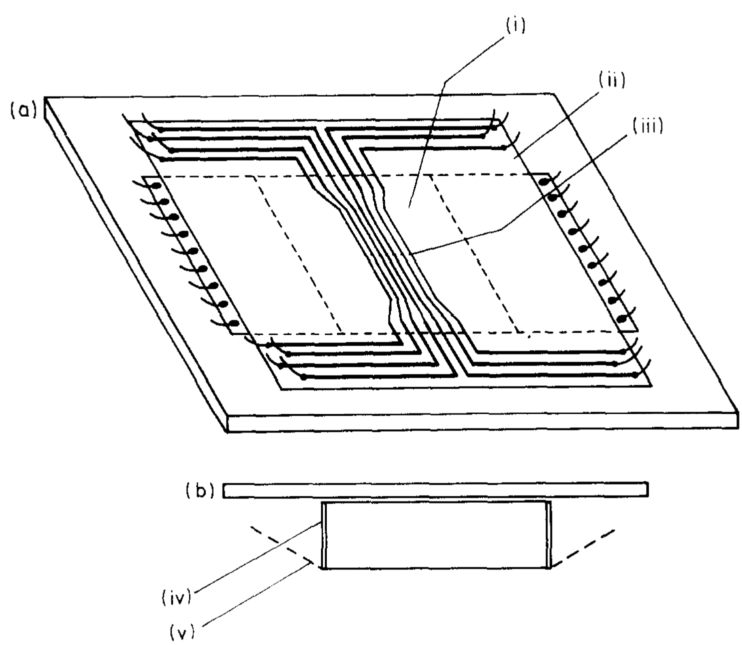

FIG. 5. Sketches of heater plate with thermometers; (a) facing upward; (b) inverted, with 'trap' for hot stratified liquid. (i) nichrome surface heater; (ii) insulating layer (silicon oxide); (iii) germanium resistance thermometers (spacing approx. 1 mm); (iv) transparent 'trap'; (v) supporting bracket.

lyses suggested that there would be little movement, provided the heating time was less than about one second. It proved desirable to have substantially longer heating time for a few tests, and for those the experiment was replanned in an inverted position, that is with the heating surface facing downwards. In addition a transparent 'box' was made by gluing four microscope slides together as shown in Fig. 5(b), to create a region below the heater in which stratified hot liquid could be trapped for a reasonably long period. Heating periods of up to 50 s were obtained by these means. The prolonged electrical input required for the longer heating period could, in principle, be obtained by adding further stages of capacitors, but they would become inconveniently large. Instead, after the last capacitor stage, a variable voltage source was connected through a resistor and diode, the voltage being initially set to a value which would cause the power supply to continue nearly proportional to $1/(\text{time})^{1/2}$, up to a period of some 5 s. Thereafter the variable voltage was adjusted by hand, to hold constant the heater temperature as observed by a thin film thermometer and displayed on a suitable instrument. By these means, thermal boundary layers several millimetres thick could be generated.

Cine photographs were taken, usually at 500 frames/s, with the camera slightly above the working surface of the heated wall, its axis at about 1° to that wall. Inside the thermal boundary layer, temperature gradients caused strong curvature of light paths, causing distortion of the image of the bubble near the wall, and generally producing a 'mirage' effect. Tests showed that, as simple ray tracing would suggest, the mirage acted very much like a mirror placed at about the top of the thermal boundary layer, preventing observation inside that layer. These problems must have been present but not recognized in many experiments reported in the literature. They arose here for the first time in our series of tests. Care was taken to preserve the datum for measurements of heights normal to the wall, by recording the position of the bubble triggering point relative to the front edge of the heated plate, before the heater was switched on. That edge was always clearly observable through isothermal, undistorting liquid. Short-lived departure, if it occurred (e.g. in negative gravity) could not be observed. Measurement of the diameter of the base of the bubble was impossible. The situation is shown in Fig. 6.

The tests were conducted with hexane, which is convenient as it is electrically non-conducting and boils at reasonable temperature and pressure. It would clearly be highly desirable to change to a different fluid with significantly different properties. Isopropyl alcohol was tried, as it has been by other experimenters, because of its significantly higher viscosity. However, it proved difficult to avoid contamination by water from the atmosphere, which caused significant electrical conduction, bypassing the electrical circuits in the liquid and also electrolysing away the thin films. No useful results were obtained. Water is another obvious candidate, but it would create worse problems of the same kind.

EXPERIMENTS

Tests were conducted in a jacketed test vessel which was mounted on a table which could be released to fall freely for a distance of about 300 mm, as shown in Fig. 1. The inner test vessel was an inverted glass bell jar containing the test fluid with various thermometers immersed in it, together with a flat glass plate. On one surface of the glass plate there were deposited in layers, the thin film heater, silicon oxide insulation and resistance thermometers, as sketched in Fig. 5. A bubble could be nucleated to grow at that surface provided the temperature immediately around it was sufficiently above the saturation temperature for the prevailing pressure. The inner vessel was surrounded by the jacket which had flat glass outer faces to facilitate observation and contained heavy paraffin and a controlled heater. By these means, any chosen bulk temperature could be maintained in the inner test vessel with little variation in time or position.

In a typical experiment a chosen temperature was first established throughout the jacket and inner test vessel, then the pressure in the inner vessel was reduced to its required value, generally at or above saturation pressure for that temperature. If necessary the pressure could be further reduced, creating super-saturation ('superheat') which could be maintained for some

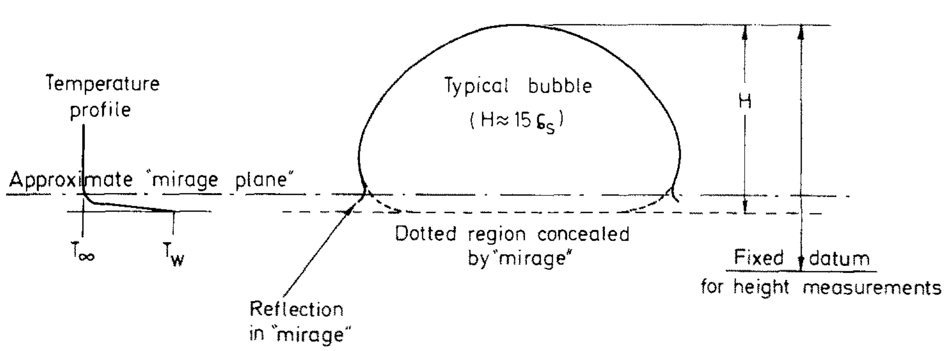

FIG. 6. Effect of 'mirage', altering and partly concealing bubble shape.

seconds provided the system had been boiled for a long time previously to remove dissolved gases and other sources of nucleation of bubbles. In such cases the tests had to follow quickly, before convection currents could percolate down from the free surface where evaporation would be taking place. In all tests, the remaining stages were under the control of an automatic sequencer which, at appropriate preselected times, switched on the camera and ultraviolet recorder, started the transient heater, released the table and initiated the bubble. The camera was normally operated at 500 or 1000 frames/s. The ultraviolet recorder at 750 mm/s recorded signals from the thin film resistance thermometers lying on the insulation above the heater. The bubble was initiated at a selected time by a local hot spot, produced by passing a timed electric pulse through a spare resistance thermometer. It was convenient to have the camera and lights stationary, a prism and lens on the table created an image of the bubble at infinity below the prism, as indicated in Fig. 1, so the camera could be focussed on infinity and remain in focus throughout the fall.

Acceleration of the table was observed in separate calibration tests, in which a steel ball was projected into slow movement relative to the table just as the table was released. Acceleration of the ball relative to the table could be measured accurately and it indicated the residual gravitational field on the table. In the free-fall tests, air resistance caused a residual field of about 0.4% of earth gravity (0.04 m/s^2). That residual acceleration could be reduced to less than one quarter by suitable arrangement of a counter-weighted accelerating (or retarding) linkage below the table. That linkage could also impose accelerations creating from +4% to −1% of earth gravity. It was not known at first whether the residual acceleration of 0.4% was sufficiently low. During our maximum bubble life of 250 ms that acceleration corresponds to a distance ($\frac{1}{2}at^2$) of approx. 1 mm, which is reassuringly small compared with sizes of our bubbles. To confirm that it could be regarded as zero gravity, some tests were made with that acceleration in the positive and negative directions.

Further details of the experimental apparatus and techniques are given in [6].

RESULTS

In all, some 250 successful tests were carried out and they can be usefully listed in categories as shown in Table 1.

It was readily observed that the bubbles showed

Table 1

	Saturation boiling	Subcooled boiling
Zero gravity	79	16
Positive gravity	31	26
Negative gravity	18	5

some general characteristics similar to those reported [1] for bubbles in initially uniformly superheated liquid; they tended to have hemispherical shape early in their life (especially if growing fast), then rounded off later. However, certain new features were also apparent, including unequivocal departure from the wall, even in zero gravity, which had never been convincingly observed in uniformly superheated liquids at zero gravity [1].

As explained above, testing started on the simplest case, namely zero gravity and saturated bulk temperature, and thereafter the complications of gravity and bulk subcooling were introduced, as discussed below.

ANALYSIS OF RESULTS

Rate of growth in zero gravity

An attempt was made to find a simple recipe for the growth of a bubble throughout its life, despite change of shape, similar to that found for bubbles in initially uniformly superheated liquid. For those, as reported in [1, 7], it has been found that the equation

rate of growth of volume of bubble

$$= \text{surface area of bubble} \times Ja\sqrt{(\alpha/t)} \quad (1)$$

gave an accurate description of volumetric growth rate. In fact the quantity $b = \sqrt{t}(\mathrm{d}V/\mathrm{d}t)/A$ was always in the range 1.0–1.2$Ja\sqrt{\alpha}$.

Several extensions of that were tried for the present experiments using estimates of the (unobservable) base area, such as

rate of growth of volume of bubble

$$= \text{base area of bubble} \times Ja_w\sqrt{(\alpha/t)}$$

but no simple expression could now be found to fit the results, even for saturated boiling. With subcooled boiling, the analogous expression might be expected to be:

rate of growth of volume of bubble

$$= (\text{curved area} \times Ja_b + \text{base area} \times Ja_w)\sqrt{(\alpha/t)}$$

and that too was tried without success. Attempts were made to incorporate simple empirical constants or to define the distinction between curved area and base area in such a way as to fit the observed growth but they become complicated without significant success. The problem was compounded by the 'mirage' effect, which prevented precise determination of the base radius.

A computation was developed in which the bubble was assumed to be hemispherical, with the curved surface behaving like a spherical bubble growing into a non-uniform temperature field (following Skinner and Bankoff [8]) and the flat base had a microlayer (analysed as in [9]). It is described in detail in [6] where it is shown to apply reasonably well for early growth. It ceased to apply when the bubble started to round off, which was shown to occur, as expected, when inertia stress $\frac{1}{2}\rho\dot{R}^2$ ceased to dominate surface tension stress $2\sigma/R$ and gravity stress $\sigma g R$. It did not lead to any simple recipe for growth of a bubble throughout its liefetime.

The current problem therefore seems to lack one of the very powerful simplifications of the case with uniformly superheated liquid, where it could be argued that, since growth was described by equation (1), the only information needed from the energy equation was the value of $Ja\sqrt{\alpha}$, hence the remaining problem was purely fluid mechanics. In that case, dimensional analysis showed that any dimensionless observed quantity would necessarily fe a function of $(Ja\sqrt{\alpha})$, ρ, μ, σ, t and hence it would necessarily be a function of two dimensionless groups, conveniently taken as

$$\frac{Ja\sqrt{\alpha}}{\sqrt{(\mu/\rho)}}, \frac{t}{Ja^6\alpha^3(\rho/\sigma)^2} \quad \text{which are} \quad \frac{Ja}{\sqrt{Pr}}, t^+.$$

Experimental results [1] for the case of uniform initial superheat did agree with that prediction, as was shown principally by demonstrating that a shape factor (D/H) was a unique function of t^+, which suggested (though did not prove rigorously) that t^+ is important and the other group $(Ja/\sqrt{Pr})$ is not. That finding will prove the starting point for our discussion of shape, below. In fact t^+ has a clear physical basis because low t^+ implies that inertia stress $(\frac{1}{2}\rho\dot{R}^2)$ is much larger than surface tension stress $(2\sigma/R)$ and high t^+ implies the opposite. The apparent unimportance of the group $Ja/\sqrt{Pr}$ implied that viscosity is not important for (D/H).

No such simple arguments can be applied here. It cannot be argued, and it may not be true, that $Ja\sqrt{\alpha}$ is the only relevant parameter from the energy equation. Hence there is no formal justification for expecting the new results to fall into a pattern in terms of t^+.

Nevertheless, the present experiments are a one-parameter variant of those in uniform superheat, differing only in having a finite value δ_s for the thermal boundary layer instead of having δ_s effectively infinite. The results were therefore plotted against t^+ in various ways, to see how they deviated from those for uniform superheat ($\delta_s = \infty$).

In uniform superheat, with growth described by equation (1), our remaining interest had centred on change of shape and hence on (D/H). In the present work, growth is much affected by δ_s, so we are now interested in graphs of D and H individually, showing their variation with time. These were put in non-dimensional form using again the groups $(Ja\sqrt{\alpha})$, ρ, μ, σ, and choosing to omit μ since viscosity had been found unimportant in [1] as stated above. That gave uniquely

$$D^+ = \frac{D}{Ja^4\alpha^2\,\rho/\sigma} \quad \text{and } H^+ \text{ similarly, (also } \delta_s^+)$$

which are plotted against t^+ in Fig. 7. There the dotted lines are derived from [1], for bubbles grown into uniformly superheated liquid, and show D^+ and H^+ following their own individual curves, initially approximately $6\sqrt{t^+}$ and $3\sqrt{t^+}$, respectively, finally both approximately $4\sqrt{t^+}$. These correspond to initial hemispherical growth with $R \approx 3\,Ja\sqrt{(\alpha t)}$ and final spherical growth with $R \approx 2\,Ja\sqrt{(\alpha t)}$, as discussed in [1]. It should be noted that the basis in [1, 7] was slightly different, using $D^* = D/(b^4\rho/\sigma)$ etc., but b is always close to $Ja\sqrt{\alpha}$ as stated above, and the discrepancy has little effect on the positions of the dotted lines.

The full lines on that figure are for three typical bubbles of the present tests, with thermal boundary layer of thickness δ_s. They were chosen to cover the full range accessible to our tests; the one furthest to the right involved inverting the heating plate to permit extended heating time, as discussed earlier. The effect of δ_s is presumably small if $H \ll \delta_s$ ($H^+ \ll \delta_s^+$), but we

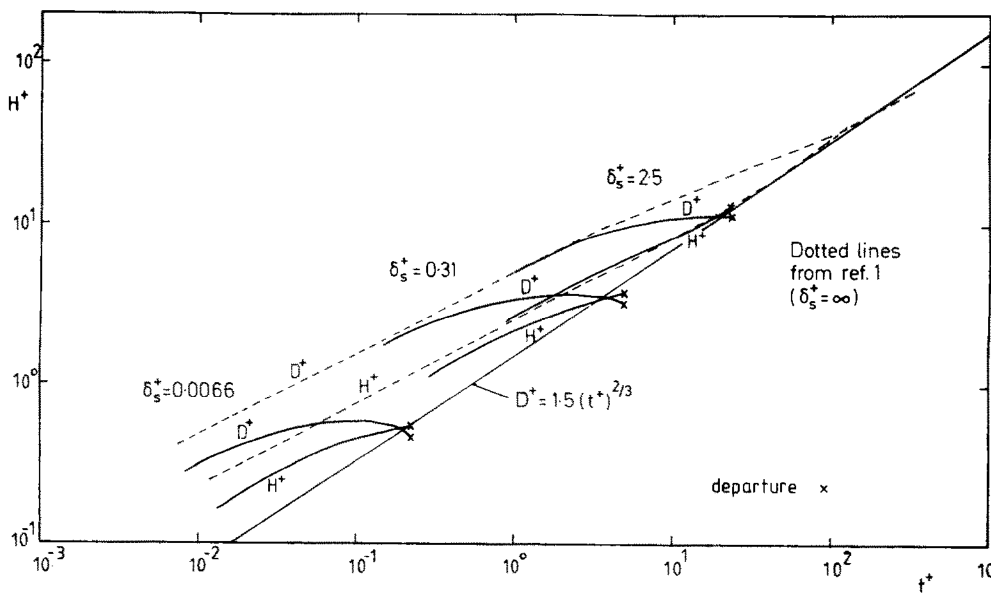

FIG. 7. Growth of bubbles in zero gravity, affected by δ_s.

can see the effects as H^+ and D^+ increase. The curves all deviate from the dotted curves obtained with uniform superheat, and all end with departure. The departure points (×) are observed to lie very close to a line $D^+ = 1.5\ (t^+)^{2/3}$, which will be discussed later.

The curves fall into a pattern, suggesting that behaviour is indeed expressible as a function of t^+ and δ_s^+. Transition from the left of the diagram to the right is controlled by the parameter δ_s^+ (if, for example, we use δ_s instead of δ_s^+, then that control is lost).

The behaviour of D^+ varies widely for different parts of the graph (different values of δ_s^+). For curves on the right (large δ_s^+), D^+ increases initially at a rate similar to that for $\delta_s^+ = \infty$ (near the dotted line), then it slows down and, if still regarded as proportional to $(t^+)^n$, then n is falling rapidly below $\frac{1}{2}$, but D^+ continues to grow almost until departure. For curves on the left (small δ_s^+), D^+ increases initially at a rate less than that for $\delta_s^+ = \infty$ (below the dotted line). This suggests that the finite value of δ_s has already had an effect, as might be expected since $\delta_s^+ = 0.0066$ and D^+ has already reached 0.3 when the bubble was first observed. D^+ then reaches a definite maximum at some time before departure, and falls well below that maximum at departure.

The behaviour of H^+ also varies according to δ_s^+, but not so much. For curves on the right (large δ_s^+), its growth rate remains close to that for $\delta_s^+ = \infty$ throughout its life, and thus H^+ is nearly proportional to $(t^+)^{1/2}$. For curves on the left, (small δ_s^+) we find, as for D^+, growth rather less than for $\delta_s^+ = \infty$, because H^+ exceeds δ_s^+ when the bubble is first observed. H^+ continues to increase, but deviates from $(t^+)^{1/2}$ and may for a limited time approximate to $(t^+)^n$, with n about 1/3.

These variations may explain the wide variety of expressions given by earlier experimenters for rate of growth of bubbles. It may be possible to explain their differences as due to their working in different parts of this complex field, though in most such experiments there were additional factors such as interacting bubbles which could add further complications.

Change of shape in zero gravity

Although the three full curves in Fig. 7 are of different form, they show similar forms for the vari-

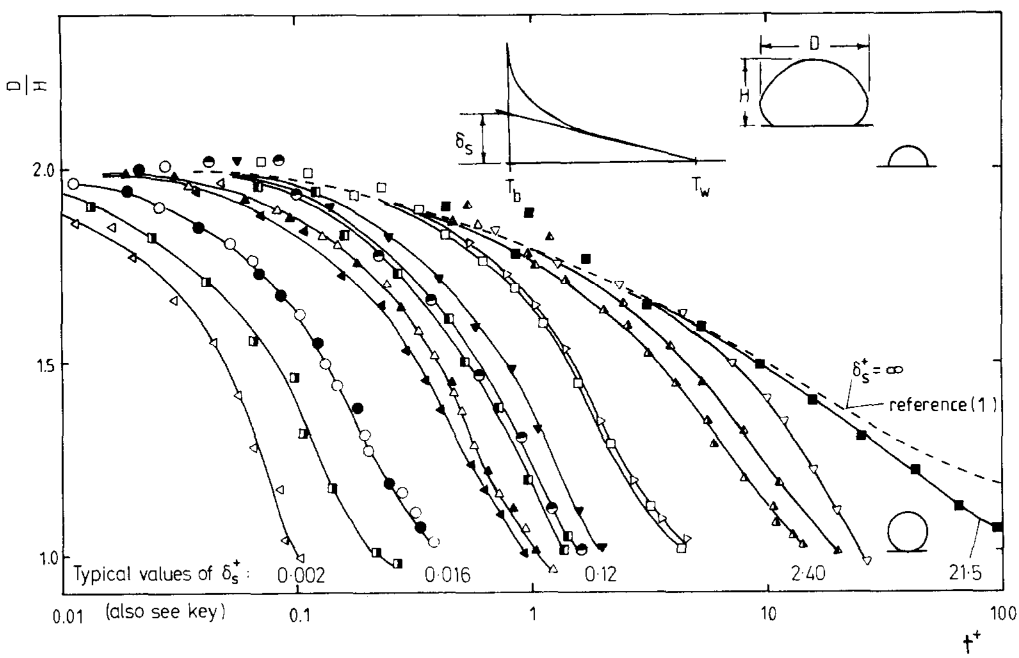

FIG. 8. Change of shape of bubbles in zero gravity, affected by δ_s. Departure occurs at the end of all curves except the last (■).

Key for this figure and Fig. 9:

◁	0.1010	0.0020	◓	0.3352	0.0768
◨	0.2446	0.0085	▼	0.2430	0.1192
●	0.3262	0.0158	□	0.4450	0.3098
○	0.1299	0.0158	▶	0.4183	0.3600
◀	0.1083	0.0414	▲	1.4253	2.404
▲	0.4247	0.0655	▲	1.5430	2.450
△	0.1276	0.0658	▽	2.8235	3.720
◧	0.3371	0.0737	■	2.7573	21.520

ation with time of the ratio D/H (the height between D^+ and H^+ curves on that log graph). That similarity is confirmed on Fig. 8 where the many curves of (D/H) for various values of δ_s^+ are all of similar shape—curves for small values of δ_s^+ lie to the left, for larger values to the right. By reading from each curve the quantity t_D^+ which is the value of t^+ corresponding to departure (or t^+ corresponding to some chosen value for D/H, say $t_{1.5}^+$), a graph of that selected t^+ against δ_s^+ could be drawn. Plotted logarithmically, such graphs proved to have a slope close to 3/4, and that was confirmed by plotting all values of D/H against $t^+/(\delta_s^+)^{3/4}$, which were then found to lie very close to a common curve (Fig. 9). Thus, for saturation boiling in zero g, our experiments show that the shape is a function of $t^+/(\delta_s^+)^{3/4}$ ending at departure as a slightly prolate spheroid ($D/H = 0.9$).

Chronologically, this was the first pattern to be noticed among our data, and it provided an encouraging indication of the continued value of our non-dimensional representation, based on $(Ja\sqrt{\alpha})$, ρ, and σ. This particular pattern, dependence on $t^+/(\delta_s^+)^{3/4}$, is a curious phenomenon. In dimensional terms this group is

$$\frac{t}{\delta_s^{3/4}}\left(\frac{\rho h_{fg}}{\rho c_p \Delta T}\right)^3 \times \frac{\sigma^{5/4}}{\alpha^{3/2}\rho^{5/4}} \quad \text{where } \Delta T = T_w - T_{sat} \quad (2)$$

which has no obvious physical basis. We therefore examined as far as possible the validity of (2) under variation of individual properties, and that reconfirmed its structure, as detailed in the appendix. We also made strenuous efforts to find any experimental limits of its validity.

To seek those limits we extended the range of experimental variables as far as practicable with our apparatus, thus exploring and extending the ranges of Figs. 7 and 8. Details of the ranges are given in the Appendix.

Extending to the left in Figs. 7 and 8 would imply smaller δ_s^+ and t^+, obtainable either by smaller heating time and bubble life-time (but life-times of less than a few ms could not be used, because of limitations from bubble nucleation and, less fundamentally, camera speed), or by high Ja (limited by attainable superheat and vacuum, and by permissible maximum size of bubble). Using small times and high Ja, that end of the range was explored without revealing any new trends. The relation seems to apply indefinitely to the left, subject always to the limitation that at very short times and fast growth rates inertia in the liquid will significantly affect pressure and saturation temperature in the bubble and we no longer have diffusion-controlled bubbles.

Extending to the right in Figs. 7 and 8 is of greater interest, partly because most industrial applications lie there and partly because the dotted curves ($\delta_s^+ = \infty$) on both Figs. 7 and 8 provide upper limits which could be expected to impinge on the shapes of the curves as δ_s^+ goes well above 1. Extension in that direction was obtainable either by long bubble life-time (limited to 250 ms, our maximum free-fall time) or by low Ja (limited by the smallest permissible size of bubble), or by large δ_s. To obtain large δ_s requires a long heating

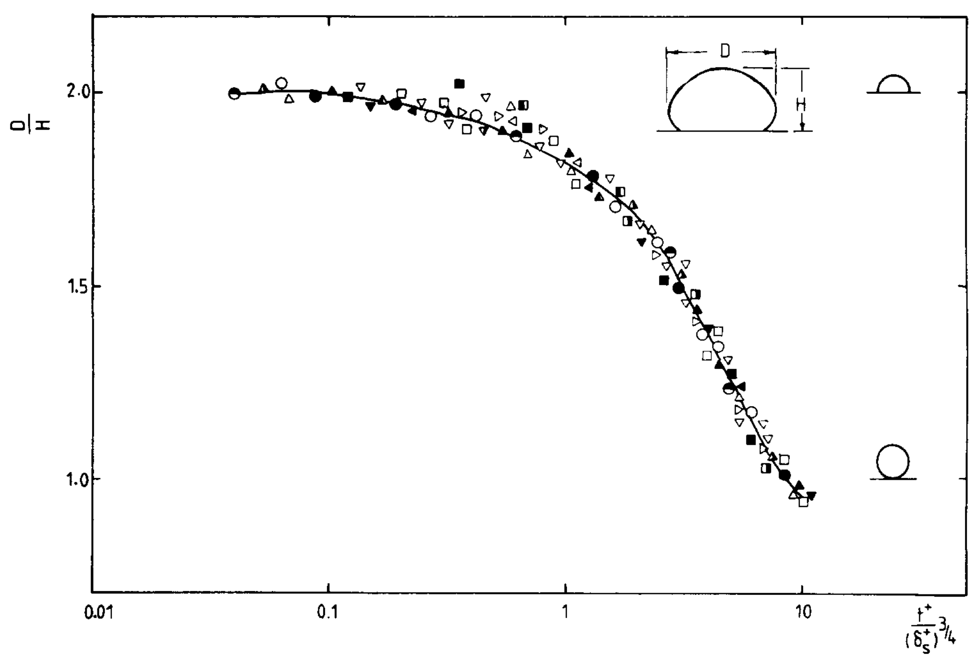

FIG. 9. Change of shape of bubbles in zero gravity, governed by $t^+/(\delta_s^+)^{3/4}$. Departure occurs at the end of all curves except ■. Key on Fig. 8.

time, to enable the thermal boundary layer to diffuse to a greater thickness. However, with heating times greater than about 1 s, serious problems with natural convection were expected, so the experiment was re-planned in an inverted position, as described earlier, to permit heating times up to 1 min, and thus give δ_s of several millimeters. This change enabled δ_s^+ to be increased from 3 to about 20. Even for these cases, the effect of the impingement on the upper limit on Fig. 8 ($\delta_s^+ = \infty$) did not much affect the curve of D/H against $t^+/(\delta_s^+)^{3/4}$, and, in particular, departure again occurred when $t^+/(\delta_s^+)^{3/4}$ is approximately 10, though there is some uncertainty because optical distortion affected the measurement of H differently in these cases from other cases.

It would, of course, have been highly desirable to have used radically different fluids, such as water, in some of our tests, but, as discussed earlier, electrical conductivity in our test fluid was unacceptable, and that precluded water or even isopropyl alcohol.

We therefore conclude that, for the experiments using hexane accessible with our techniques, for bubbles in zero gravity with saturation bulk temperature, the shape is a function of the group $t^+/(\delta_s^+)^{3/4}$. The result is purely experimental. Its form is curious. It was reached by extension of the analysis for bubbles in uniformly superheated liquid, but there is no formal justification for that extension.

Parameters at departure in zero gravity

As indicated by Figs. 8 and 9, departure occurred for all of these bubbles when D/H was approximately 0.9 and $t^+/(\delta_s^+)^{3/4}$ was approximately 10. Hence there is a relation for departure time for isolated bubbles in saturation boiling in zero gravity, as follows:

$$t_D^+/(\delta_s^+)^{3/4} \simeq 10 \text{ or } t_D \simeq 10\,\delta_s^{3/4}\,Ja^3\,\alpha^{3/2}\,(\rho/\sigma)^{5/4}.$$

For the size of these bubbles at departure, a further purely empirical result can be reached [6] as follows:

$$D_D^+/(\delta_s^+)^{1/2} \simeq 7 \text{ or } D_D \simeq 7\,\delta_s^{1/2}\,Ja^2\,\alpha\,(\rho/\sigma)^{1/2}.$$

From these we can recover the relationship mentioned earlier and shown by the line on Fig. 7

$$D_D^+ \simeq \frac{7}{10^{2/3}}(t_D^+)^{2/3} \simeq 1.5\,(t_D^+)^{2/3}$$

or

$$\frac{D_D}{t_D^{2/3}} \simeq 1.5\left(\frac{\sigma}{\rho}\right)^{1/3} \tag{3}$$

which implies that, for saturation boiling if gravity is negligible, $D_D/t_D^{2/3}$ is independent of growth rate $(Ja\sqrt{\alpha})$ and of δ_s and also almost independent of fluid since $(\sigma/\rho)^{1/3}$ varies very little for normal fluids (organics, water, refrigerants, even cryogens, except He).

At departure, the shape is approximately a prolate spheroid with $D/H = 0.9$, so the volume is approximately $(\pi/6)\,D_D^3/0.9$, hence

$$\frac{V_D}{t_D^2} \simeq 2.0\frac{\sigma}{\rho}.$$

These last results are so remarkably simple and universal that it may be hoped they will form a starting base for improved understanding of the relation between departure diameter and bubble frequency. Comparison of relation (3) with a scatter plot of departure diameter against bubble frequency f [10] suggests that (3) may yield an upper bound, in the form

$$D_D f^{2/3} < 1.5\,(\sigma/\rho)^{1/3}$$

on that plot. That is to be expected because f is $1/(t_D + t_w)$, where t_w is waiting time, so $f < 1/t_D$.

Effect of gravity

Having established the curves of Figs. 7–9 as a 'norm' for zero gravity, we were able to restore gravity (positive or negative, earth gravity or fractional, perpendicular or parallel to the wall) and look for divergence from that 'norm'. That had already been done for bubbles growing into uniformly superheated liquid, as described in [1], where it was shown that behaviour in earth or fractional gravity depended on a non-dimensional group involving gravity, again non-dimensionalized by use of $(Ja\sqrt{\alpha})$, ρ, σ, which gave $g^+ = gJa^8\alpha^4\,(\rho/\sigma)^3$. It was found there that, for fast growing bubbles with positive g (buoyancy assisting departure)

$$\begin{aligned} t_D^+(g^+)^{2/3} &= 4 \quad \text{or} \quad t_D[g/(Ja\sqrt{\alpha})]^{2/3} = 4 \\ D_D^+(g^+)^{1/3} &= 12 \quad \text{or} \quad D_D[g/(Ja^4\,\alpha^2)]^{1/3} = 12 \end{aligned} \tag{4}$$

where both numerical constants must be reduced for slower growing bubbles. There, interest centred on shape and departure, but we are now interested in more detail. For those bubbles, more details were given in [7], from which we produce the three curves shown in Fig. 10. The dotted lines are as in Fig. 7, showing the variation of D^+ and H^+ in zero gravity. The three curves show effects of gravity, controlled by the parameter g^+, and ending in departure, in accordance with equation (4) above.

We now wish to consider cases where both gravity and thermal boundary layer are present, and we expect the results to vary between those in Fig. 10 (gravity but no thermal boundary layer) and in Fig. 7 (thermal boundary layer but no gravity). The matter becomes complicated, and it must be recognized that a relation must be accurate and yet simple [like (3) above] if it is to be useful in practice.

Clearly, crucial questions are: when does one mechanism or the other predominate, and what happens if both are significant? The question can be partly answered at this stage, and we first seek criteria for deciding whether we have the extreme cases

(a) where effects of δ_s^+ are dominant, so the zero g expressions should be used (3);
(b) where effects of gravity are dominating, so the g^+ expressions should be used (4).

Indeed, it was essential to find criterion (a) in order to establish how low the acceleration of the table must be for 'zero gravity'.

It seems a natural presumption that, if one mechanism predicts departure time and size both much less than the other predicts, then the former mechanism is predominant. For δ_s to predominate over g, the time criterion is more severe (i.e. if the time criterion is met, then so is the size criterion), and that can be written

$$10\,(\delta_s^+)^{3/4} = t_{D_\delta}^+ \ll t_{D_g}^+ = \frac{4}{(g^+)^{2/3}}$$

hence

$$(g^+)^{2/3}\,(\delta_s^+)^{3/4} \ll 0.4 \qquad (5)$$

or

$$g^{2/3}\,\delta_s^{3/4}\,b^{7/3}\,(\rho/\sigma)^{5/4} \ll 0.4.$$

For g to predominate over δ_s, the size criterion is more severe and that leads to

$$(g^+)^{1/3}\,(\delta_s^+)^{1/2} \gg 12/7$$

or

$$g^{1/3}\,\delta_s^{1/2}\,b^{2/3}\,(\rho/\sigma)^{1/2} \gg 12/7. \qquad (6)$$

Of course, with inequalities 'much greater' or 'much less', we immediately ask how much? From these experiments, that can be answered for δ_s predominant [case (a) above]: if $t_{D_\delta} < (t_{D_g}/10)$, then gravity has little effect, as was confirmed by running pairs of tests, identical except that gravity was reversed ($g = \pm 0.004\,g_e$). So we have a criterion for negligible gravity, which is

$$(g^+)^{2/3}\,(\delta_s^+)^{3/4} < 0.04$$

or

$$g^{2/3}\,\delta_s^{3/4}\,b^{7/3}\,(\rho/\sigma)^{5/4} < 0.04.$$

Among the present experiments, there are no cases in which the effects of gravity predominate over δ_s. In fact the criterion suggested above (6) can be rearranged as

$$Ja^{2/3} \gg \frac{12}{7}\,\frac{1}{g^{1/3}}\,\frac{1}{\delta_s^{1/2}}\left(\frac{\sigma}{\rho}\right)^{1/2}\frac{1}{\alpha^{1/3}}.$$

If we now assume the thermal properties of hexane, earth gravity, $\delta_s = 1$ mm, and again assume that $\gg$ implies a factor 10, we obtain $Ja > 5500$. That value is virtually unattainable, and if attained it would give, not diffusion-controlled, but inertia-controlled bubbles.

In fact, the only cases in which g predominated were those arising from Pike's experiments [1], in which there was no thermal boundary layer present. Further investigation is needed, and we must bear in mind that these experiments relate to a limited range of fairly large Jacob numbers, but it may emerge that, when a thermal boundary layer is present (as it is in practice), gravity rarely predominates in the mechanism of departure.

In many of our tests, both mechanisms were significant. The observed departure time was then less, often much less, that those predicted by either mechanism acting alone. Curves of D^+ and H^+ for two such tests are shown in Fig. 11, accompanied in each case case by the curves to be expected if gravity were absent and if δ_s were infinite. Clearly, t_D is lower than would be expected with δ_s alone or with g alone. The curves on the right of Fig. 11 suggest that, if that reduction in t_D is small, then D_D may be larger than in

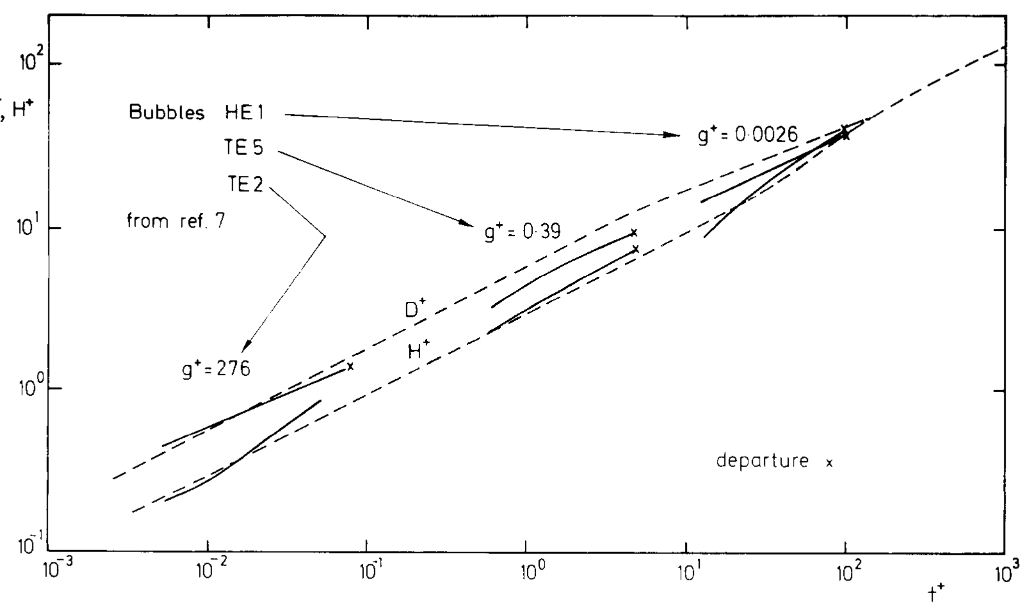

FIG. 10. Growth and departure of bubbles in initially uniformly superheated liquid ($\delta_s = \infty$), affected by gravity (Refs. [1, 7]).

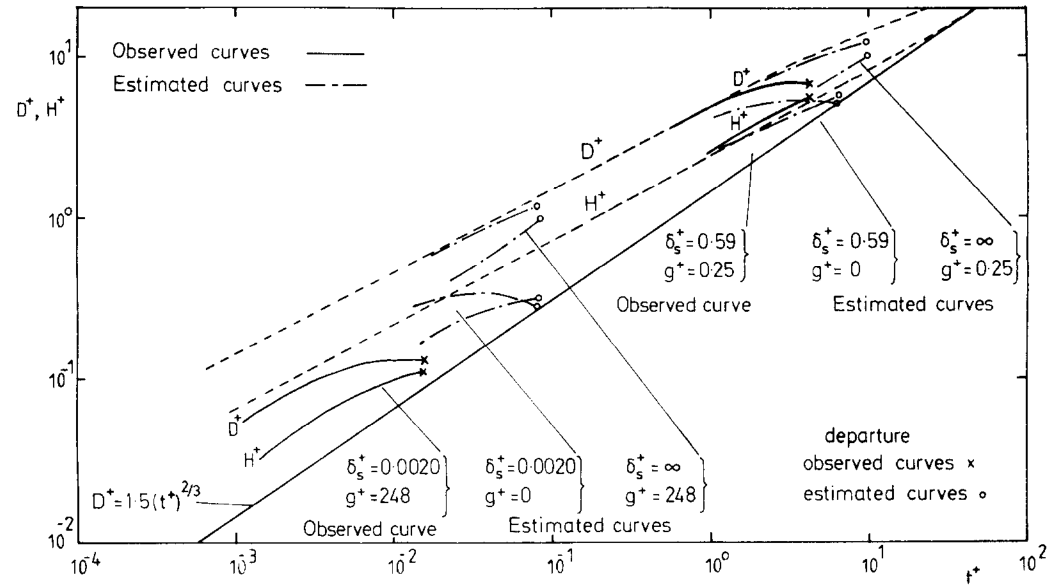

FIG. 11. Growth and departure of bubbles affected by thermal boundary layer (finite δ_s) and by gravity.

zero g; it may seem odd that gravity increases departure diameter, but it is consistent with the peaked curves for D^+ shown in Fig. 7. We might speculate that gravity has caused warm liquid to rise around the bubble, or perhaps that the change to prolate shape (D falling relative to H) has been cut short.

It therefore seems that there will be a continuous pattern of change along these lines, from dominance of δ_s towards (though perhaps rarely reaching) dominance of gravity. The representation in Fig. 11 is probably as simple and concise as can be attained, but it still does not lend itself to simple algebraic approximations. The criterion for δ_s to predominate can be rewritten (though perhaps not very helpfully) as

$$\delta_s < \frac{\{\sigma/(\rho g)\}^{8/9}}{\{250 Ja^4 \alpha^2 \rho/\sigma\}^{7/9}}$$

in which $\sigma/(\rho g)$ is recognisable as the square of the characteristic length L_m for meniscus problems [$L_m = \sqrt{(\sigma/\rho g)}$] and $250Ja^4\alpha^2\rho/\sigma$ is (less recognizably) a characteristic size for bubble rounding by surface tension; in fact it is approximately the diameter of a bubble as it becomes nearly spherical ($D/H = 1.05$) when grown into uniformly superheated liquid in zero gravity, as can be derived from [1].

To consider the effect of gravity on shape, we start from Fig. 9 which showed the unique dependence of D/H on $t^+/(\delta_s^+)^{3/4}$ in zero gravity. Results of tests with and without positive (buoyant) gravity were plotted against $t^+/(\delta_s^+)^{3/4}$ as shown in Fig. 12, in which the zero gravity cases of Fig. 9 are represented by a single curve ($g^+ = 0$) and other curves show effects of increasing g^+. Those curves again show much the same form, suggesting that they are unique functions of

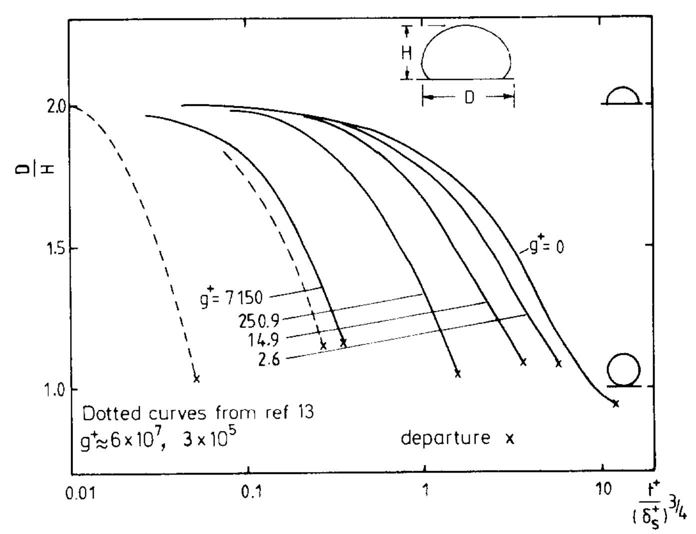

FIG. 12. Change of shape of bubbles with $t^+/(\delta_s^+)^{3/4}$, affected by gravity.

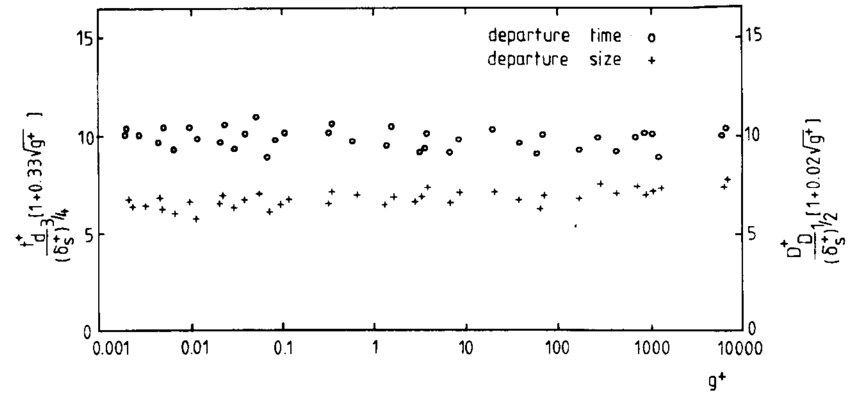

FIG. 13. Expressions for time and size at departure, affected by thermal boundary layer (finite δ_s) and by gravity.

some suitably modified time variable. After some trials, it emerged that, within the range of our tests (gravity never truly predominant), the change in shape and departure of isolated bubbles in saturation boiling in positive or zero gravity was well represented by a unique function of the variable $[t^+/(\delta_s^+)^{3/4}]$ $(1 + 0.33\sqrt{g^+})$, and that new variable again had the value 10 at departure. For diameter at departure, a similar analysis was made, giving

$$\frac{t_D^+}{(\delta_s^+)^{3/4}}(1+0.33\sqrt{g^+}) \simeq 10 \qquad (7)$$
$$\frac{D_D^+}{(\delta_s^+)^{1/2}}(1 + 0.02\sqrt{g^+}) \simeq 7$$

as shown by Fig. 13, though again there is no formal justification. Due to unattainability of the fully gravity-dominated case, these results could not be linked to those for initially uniformly superheated liquid, quoted above (4), and they must be confined to the range of the experiments. There is some indication from other workers (below) that they may not apply for much faster growing bubbles.

Tests with the plate inverted or in normal orientation but with the table accelerating down faster than 9.81 m/s^2 gave 'negative', non-buoyant, gravity, tending to hold the bubble at the plate. Nevertheless, departure was observed as described in [6], provided g^+ was sufficiently small, and/or other factors favouring departure were present, notably thin thermal boundary layer and high subcooling. This phenomenon of departure 'against gravity', as from a downward-facing surface, has long been known to occur in developed boiling [11], but it is here observed for the first time under controlled conditions.

Effect of bulk temperature

The effect of having a bulk temperature which differs from saturation value (usually subcooled) was first

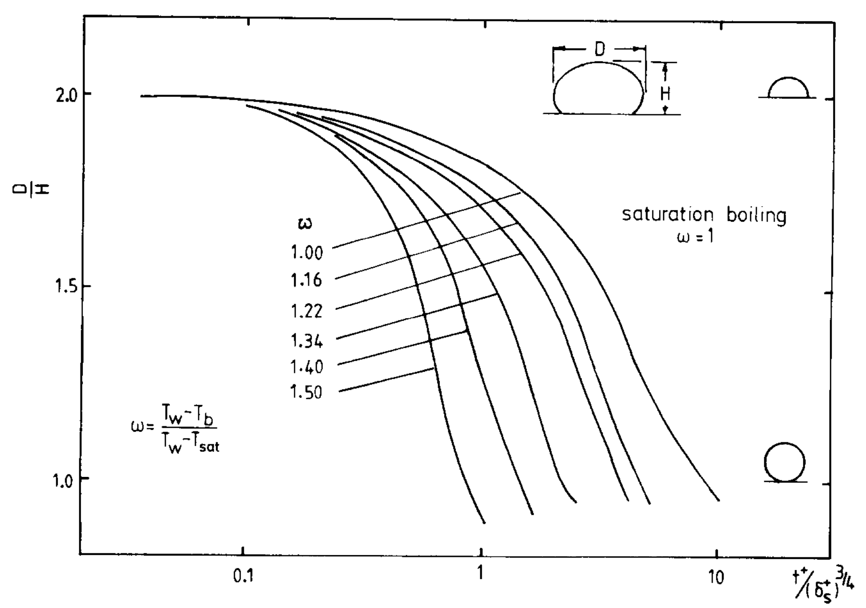

FIG. 14. Change of shape of bubbles with $t^+/(\delta_s^+)^{3/4}$, affected by subcooling.

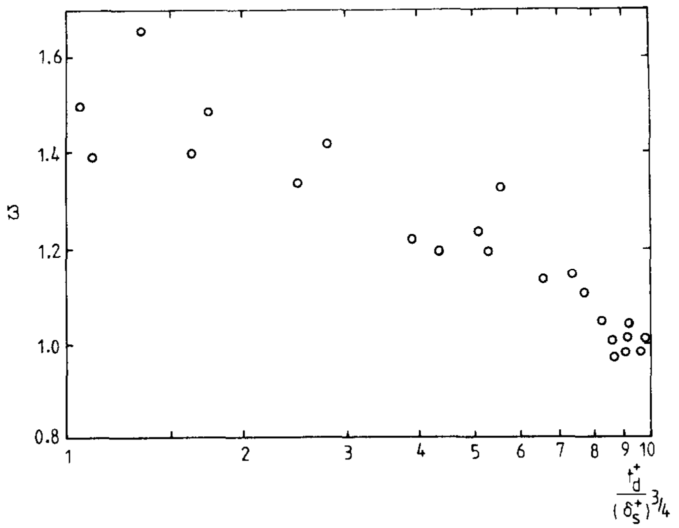

FIG. 15. Departure of bubbles in zero gravity, affected by subcooling.

examined for tests in zero gravity. The subcooling tended to reduce the departure time as indicated in Fig. 14 and 15, where it can be seen that the shape and the departure group $t_D^+/(\delta_s^+)^{3/4}$ depend on the subcooling parameter $\omega = (T_w - T_b)/(T_w - T_{sat})$. A general trend can be seen, and algebraic expressions can be set up like (7) to approximate to the trend, but the amount of scatter is now rather large and there is less confidence in any particular algebraic expression.

Combined effects of bulk temperature and gravity

The cases considered above with saturation bulk temperature or zero gravity or both will cover many applications. However, cases can arise in which there are significant effects from subcooling and from gravity. We conducted some 30 tests of that kind, and results with positive gravity are shown in Fig. 16, in terms of the effect of subcooling upon the groups $t_D^+(1 + 0.33\sqrt{g^+})/(\delta_s^+)^{3/4}$ and $D_D^+(1 + 0.2\sqrt{g^+})/(\delta_s^+)^{1/2}$, which were constant in saturation boiling. Again, trends are apparent, and, although the scatter is too large to suggest any algebraic approximation it is clear that greater subcooling leads to earlier departure.

The trend applied also when gravity was negative (non-buoyant). As mentioned above, departure 'against gravity' was favoured by greater subcooling.

General comments

The comment might be made that most of this is not surprising. We would agree—indeed we find that reassuring. What is new is that we have now quantified various effects which had previously been known (or vaguely anticipated) merely as general trends of behaviour.

Also, it was found in [1, 7] that surface tension may assist bubble departure, in contradiction of established theories. Similarly, it is found here that positive (buoyant) gravity may increase departure diameter, in contradiction of established theories. These contradictions are perhaps surprising, though they are not primarily of interest for the effects themselves, which are small. However, they are of interest as indicating the reservations needed in approaching established theories. No better theories are offered here: the matter involves very complex interactions of fluid mechanics and heat flow.

Nothing has been said, and perhaps little can usefully be said by way of analytical explanation of the phenomena, in terms of the fundamentals of fluid mechanics and heat flow. For example, it is probably true (but a truism) to say that, as the rate of growth of the bubble is reduced due to penetrating beyond the thermal boundary layer, (particularly if there is subcooling), so the consequent reduction in inertia stress encourages rounding-off and departure. It is, however, difficult to back that by analysis.

The use of our particular non-dimensional representation may seem dubious because unfamiliar. A non-dimensional representation, if it is appropriate to the problem, will have the beneficial effect of incorporating some chosen aspect(s) of the behaviour, as *Re* gives a common graph for drag coefficient on all spheres in all fluids. Our representation seems useful because it incorporates into the basic graphs (as dotted lines on Figs. 7, 10, 11) the growth as it arises without thermal boundary layer, including as well the transition from initial hemispherical shape to spherical.

No computation in this field has yet approached the complexity needed for adequate modelling of the behaviour of such bubbles, with coupled energy flow and fluid mechanics, having an unknown moving boundary, with significant effects from gravity, surface tension, perhaps thermocapillarity and (in the microlayer at least) from viscosity. The problems could be regarded as a challenge to workers interested in advanced computation of thermo-fluid-dynamics, but the large effort needed to compute this problem would appear to be greater than the value to be obtained from

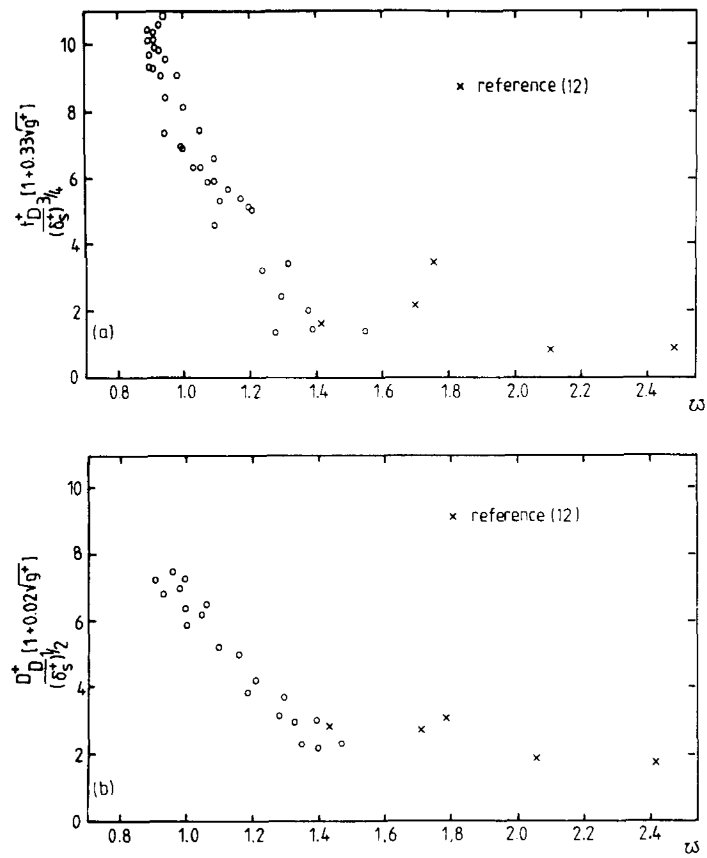

FIG. 16. Departure of bubbles, affected by thermal boundary layer and by gravity and by subcooling.

the solution. We confined our own computation to data processing and the significant but highly simplified computation of hemispherical growth. It seems that, for some time to come, this will remain a field in which careful, fundamental experiment is cheaper and more informative than computation.

COMPARISON WITH OTHER WORKERS

Few tests have been reported which can be compared with these, since most studies involve continuous boiling. Some tests have been reported in which a burst of electrical heating was applied at constant rate to a thin metallic strip in liquid, and a bubble or bubbles occurred naturally as the temperature rose. The temperature boundary layer is then not an error function, but it can be approximated to an error function for purpose of comparison. One such series is by Shrock and Perrais [12] who used water. Unfortunately their results lie in the difficult region where there are significant effects from gravity and subcooling. The results are plotted on Fig. 16 for comparison, but they generally had greater subcooling than our tests.

Tests with individually nucleated bubbles in a non-uniform temperature were reported early in the present investigations by Cooper and Lloyd [13]. The bubbles were formed at the bottom of a vessel which was continuously heated from below with known flux $(\dot{q}/A)$ and the wall temperature was measured, as here. No attempt was made to control heat loss and convection in the liquid, nor to measure the temperature profile in the liquid before the bubble was initiated, though bulk temperature was measured and was close to saturation. Assumptions must therefore be made before the results can be applied here, principally that prior movement in the liquid was negligible and that the equivalent value of δ_s is given by assuming simple conduction near the wall, so $k(T_w - T_{sat})/\delta_s = (\dot{q}/A)$. The tests were all at very low pressure, down to 1 psia, giving high Ja and correspondingly fast growth rate. These conditions produce points lying far to the left of ours in Fig. 11, but they are quite consistent with a continuation of the trends we observed. Both gravity and thermal boundary layer (but not subcooling) seem to be significant, t_D is again less than would be expected with either acting alone. The point (t_D^+, D_D^+) again lies between the two lines of Fig. 11 (extended). The shape varies, as shown in Fig. 12, in a similar manner to bubbles of this study, but the effect of g^+ is not well represented by (7). In view of the uncertainty in δ_s for these tests, the matter is not pursued further, but it lends some support to the present work.

Clearly, experiments can reach that region, the far left of Fig. 11, but, as discussed earlier, most industrial interest is on the right of that figure. That region is much harder to reach experimentally, and few experimental results have been reported.

INDUSTRIAL APPLICATION

The object of the work is to contribute toward an improved fundamental basis for correlations of boiling under industrial conditions. To be useable, any contribution from this fundamental level must be kept simple, otherwise matters will become intolerably complex when attempts are made to apply it to developed boiling, where there are many further complications of nucleation, interaction of bubbles, two-phase flow, etc. Expression (3) at least meets this requirement. On the other hand, it is counterproductive and confusing to deny complexity where it exists. It is now becoming clear that the behaviour of individual bubbles in actual boiling conditions is complicated in ways which have not hitherto been recognized, and ways which cause significant changes in the parameters (e.g. time and size at departure) which are used in existing correlations.

Tests of our type are conveniently done with Ja_w of about 15–150, which corresponds broadly to low flux nucleate boiling at pressures of about 1 atm or less, which are met in some process industries. Only by understanding and using modelling laws can we expect to understand conditions at the higher pressures encountered in boilers, where bubbles are very small.

Another study is in hand here to examine the effect of movement in the liquid before initiation of the bubble. As these studies come to fruition, their effects on existing correlations are being considered, to seek ways of improving those correlations.

CONCLUSIONS

Studies of individual vapour bubbles growing at a wall into initially stagnant liquid have been extended by introducing controlled initial temperature profiles in the liquid. Analysis has been aided by dimensional considerations and also by comparison with the even simpler case reported previously, in which the liquid was initially isothermal (uniform 'superheat').

The simplest cases newly reported here involved negligible effects of gravity (using a free-fall environment) and a temperature profile consisting of a thermal boundary layer characterised by thickness δ_s at the wall, with saturation temperature in the bulk liquid (hexane). In that case, δ_s has marked effect and various simple patterns of behaviour emerge

(1) As the bubble grows relative to the thickness δ_s, its growth is slower than in uniformly superheated liquid. A computation was set up, reasonably successfully, for early phases of growth, but it was not possible to find a simple recipe for growth at all times, such as was found for uniform superheat in [1].

(2) Bubbles depart normal to the wall with diameter and time related by

$$\frac{D_D}{t_D^{2/3}} \simeq 1.5\left(\frac{\sigma}{\rho}\right)^{1/3}$$

and with volume and time related by

$$\frac{V_D}{t_D^2} \simeq 2.0\frac{\sigma}{\rho}$$

(3) The change of shape and departure of the bubble appear to be determined by the dimensionless group $t^+/(\delta_s^+)^{3/4}$; in particular, departure occurs when that group has value about 10, so departure time t_D is given by

$$t_D = 10\,\delta_s^{3/4}\,Ja_w^3\,\alpha^{3/2}\,(\rho/\sigma^{5/4}).$$

(4) An expression for departure diameter also follows from these

$$D_D = 7\,\delta_s^{1/2}\,Ja^2\,\alpha(\rho/\sigma)^{1/2}.$$

Values of δ_s and Ja_w were varied as much as possible to confirm these results over a wide range, still with zero gravity and saturation bulk temperature. These results can be seen as a one-parameter variant of the behaviour already reported with uniform superheat in zero gravity, though in that case no departure was convincingly observed, whereas it is in the present tests.

Effects of gravity (+ or −) normal to the wall were also investigated. Joint effects of gravity and thermal boundary layer can be seen in the results, which lie in a pattern between the earlier uniform superheat tests with gravity and the tests just reported with thermal boundary layer but no gravity. The pattern covers a wide range of behaviour, which may help to sort out the wide range of published expressions for bubble growth and departure. It appears that, when a thermal boundary layer is present, the effects of gravity will rarely predominate in causing departure. Some simple analytic expressions can be obtained for combined effects of thermal boundary layer and gravity, but their validity may be confined to the range of our experiments.

Effects of subcooling were also investigated, and these analytic expressions can be modified to incorporate them, though the combined effects of thermal boundary layer with subcooling and gravity remain too complex to be followed with confidence, even in these controlled conditions.

Departure was observed to occur 'against gravity' (i.e. in negative or non-buoyant gravity, as from a downward-facing surface), as has long been reported in developed boiling. In our controlled tests it was possible to identify conditions favouring that behaviour, principally strong subcooling and thin thermal boundary layer.

Experimental difficulties with electrical conduction in the liquid have so far prevented the extension of these tests to significantly different fluids such as water. The few results from other workers which can be compared in detail appear to be consistent.

Acknowledgements—The work started at the Engineering Department, Cambridge University and was transferred to the Department of Engineering Science, Oxford University. T.T.C. acknowledges with thanks a Research Studentship at Trinity College, Cambridge. Both authors acknowledge with thanks financial support from the Engineering Sciences Division, A.E.R.E., Harwell.

REFERENCES

1. M. G. Cooper, A. M. Judd and R. A. Pike, Shape and departure of single bubbles growing at a wall. Paper PB-1, *6th International Conference on Heat Transfer*, Toronto (1978).
2. B. D. Marcus and D. Dropkin, Measured temperature profiles within the superheated boundary layer above a horizontal surface in saturated nucleate pool boiling of water, *J. Heat Transfer* **87C**, 333 (1965).
3. J. R. Weibe and R. L. Judd, Superheat layer thickness measurements in saturated and subcooled nucleate boiling, *Int. J. Heat Mass Transfer* **12**, 843 (1969).
4. K. Nishikawa, Y. Fujita, Y. Nawata and T. Nishijima, Studies on nucleate pool boiling at low pressures, *Heat Transfer Jap. Res.* **5**, 66 (1976).
5. T. E. Lippert and R. S. Dougal, A study of the temperature profile measured in the thermal sublayer of water, Freon 113, and methyl alcohol during pool boiling, *J. Heat Transfer* **90C**, 347 (1968).
6. T. T. Chandratilleke, Pool boiling—growth of single bubbles at a heated wall. Ph.D. Thesis, Cambridge University, England (1980).
7. R. A. Pike, Bubble dynamics in boiling, Ph.D. Thesis, Cambridge University, England (1976).
8. L. A. Skinner and S. G. Bankoff, dynamics of vapour bubbles in general temperature fields. *Physics Fluids* **8**, 1417 (1965).
9. M. G. Cooper and J. M. D. Merry, A general expression for the rate of evaporation of a layer of liquid on a solid body. *Int. J. Heat Mass Transfer* **16**, 1811 (1973).
10. W. C. Baron v. Ceumern-Lindenstjerna, Bubble departure diameter and release frequencies during nucleate pool boiling of water and aqueous sodium chloride solutions, Chap. 3 in *Heat Transfer in Boiling*, (edited by E. Hahne and U. Grigull). Academic Press, Hemisphere (1977).
11. N. Isshiki and H. Tamaki, Photographic study of boiling heat transfer mechanisms, *Bull. Jap. Soc. Mech. Engrs* **6**, 505 (1963).
12. V. E. Schrock and J. P. Perrais, Dynamics of bubbles in a known temperature distribution. *Proc.* 1966 *Heat Transfer and Fluid Mech. Inst.* p. 122 (1966).
13. M. C. Cooper and A. J. P. Lloyd, Transient local heat flux in nucleate boiling, *3rd Int. Heat Transfer Conf.* paper 100, Chicago (1966).

APPENDIX

Having experimentally confirmed, as far as we could, the controlling significance of the group $t^+/(\delta_s^+)^{3/4}$, we considered how far we could confirm its structure by checking the implied dependence on individual properties. Inserting the individual properties in to the group, we obtained (2), repeated here for convenience

$$\frac{t^+}{\delta_s^{+\,3/4}} = \frac{t}{\delta_s^{3/4}}\left(\frac{\rho_g h_{fg}}{\rho c_p \Delta T}\right)^3 \times \left(\frac{\sigma^{5/4}}{\alpha^{3/2}\,\rho^{5/4}}\right)$$

$$\text{where } \Delta T = T_w - T_{\text{sat}}. \qquad (2)$$

This apparently takes the value 10 at departure in zero g.

Ideally, such a statement would be checked by varying each property in turn, but of course that is impracticable here as several of the properties could not be greatly varied in our experiments, nor incidentally do they vary greatly in actual industrial practice for normal fluids, if we exclude liquid metals and also water (considered below). The principal quantities which could be varied in our experiments were δ_s, ΔT and p, the system pressure. The first two appear in the statement (2) directly, and the last one acts largely through affecting ρ_g and (slightly) h_{fg}. Hence there is the possibility of directly checking the dependence of t_D (or $t_{1.5}$ etc.) on δ_s, ΔT and the product $(\rho_g h_{fg})$, at least to the extent of checking the powers a, b, c in an expression of the form

$$t_D = K\delta_s^a\,\Delta T^b\,(\rho_g h_{fg})^c$$

where K, a, b, c are constants. Their values were found by least squares fit among $\log t_D$, $\log \delta_s$, $\log \Delta T$, $\log(\rho_g h_{fg})$, using all available data—some 55 points—with ranges as follows:

δ_s	from	0.07	to	2.8 mm
ΔT	from	9.5	to	23.1 K
$(\rho_g h_{fg})$	from	216	to	590 kJ/m^3.

The results were $a = 0.75$, $b = 2.8$, $c = -2.7$, thus clearly supporting all the verifiable parts of statement (2). The remainder of (2) amounts to

$$\frac{\sigma^{5/4}}{\rho^{11/4}\,(kc_p)^{3/2}}. \qquad \text{(A1)}$$

None of these properties varies greatly with pressure for a given fluid (remote from the critical point). Nor do they vary greatly among fluids in common use, compared with possible variation of 100 or more in ρ_g which would affect expression (2) by 10^6. In our experiments with hexane, (A1) varied little from 24×10^{-15} (SI units). Water is unusual as regards σ and c_p, and also as regards k, and the value of (A1) for water at 100°C is 1.4×10^{-15}, a reduction by factor 17. Hence the variation in these residual parts (A1) of expression (2) is smaller than that attainable by variation of ΔT and $(\rho_g h_{fg})$.

CROISSANCE DE BULLES DE VAPEUR CONTROLEE PAR LA DIFFUSION SUR UNE PAROI, DANS UN GRADIENT DE TEMPERATURE CONNU

Résumé — Des études antérieures sur la croissance de bulles individuelles de vapeur sur une paroi et dans un liquide immobile ont été étendues en introduisant un profil initial de température dans le liquide. Les cas les plus simples sont étudiés (gravité nulle, masse liquide à la température de saturation) en utilisant l'analyse dimensionnelle et en comparant avec des expériences et des analyses dans une situation plus simple, par exemple température initiale uniforme. Différentes configurations de comportement sont trouvées qui sont largement en accord les idées formées mais qui peuvent être maintenant quantifiées.

En l'absence de gravité, les bulles quittent la paroi à des tailles et des époques qui peuvent être calculées, au moins pour des bulles dans le domaine de ces conditions expérimentales. Ce domaine est étendu aussi loin que possible et il correspond à l'ébullition nucléée à la pression atmosphérique ou inférieure. Pour l'ébullition à la saturation, on obtient une relation particulièrement simple et universelle entre le temps et le diamètre (ou le volume) au départ. La relation est indépendante de la vitesse de croissance et de l'épaisseur de la couche limite thermique:

$$D_D/t_D^{2/3} \simeq 1{,}5(\sigma/\rho)^{1/3} \quad \text{ou} \quad V_D/t_D^2 \simeq 2{,}0\sigma/\rho.$$

Puisque σ/ρ ne varie pas beaucoup pour les fluides usuels, cette relation est donc faiblement dépendante du fluide.

Le phénomène bien connu des bulles se développant 'contre la pesanteur' (gravité négative comme dans le cas d'une plaque à face tournée vers le bas) est observé pour la première fois dans des conditions contrôlées et les conditions en faveur de ce comportement sont identifiées. Ce sont principalement une mince couche limite thermique et un fort sous-refroidissement.

Un résultat imprévu est que la gravité positive peut, dans certains cas, provoquer le départ d'une bulle avec une dimension plus grande qu'en l'absence de pesanteur.

DAS WACHSTUM THERMISCH KONTROLLIERTER DAMPFBLASEN AN EINER WAND IN EINEM BEKANNTEN TEMPERATURGRADIENTEN

Zusammenfassung — Frühere Untersuchungen an Einzeldampfblasen die an einer Wand in eine anfangs ruhende Flüssigkeit hineinwachsen, wurden durch die Einführung eines vorgegebenen Temperaturprofils in der Flüssigkeit erweitert. Zunächst wurden die einfachsten Fälle untersucht (Schwerelosigkeit, Flüssigkeit fern der Wand auf Sättigungstemperatur). Dimensionsanalyse und der Vergleich mit früheren Experimenten und theoretischen Untersuchungen bei noch einfacheren Bedingungen, d.h. bei anfangs einheitlicher Temperatur, wurden dabei herangezogen. Verschiedene Verhaltensformen konnten beobachtet werden — sie entsprechend weitgehend dem Erwarteten, können aber nun quantifiziert werden.

Bei Schwerelosigkeit können Abreißzeitpunkt und -größe der Blasen vorausbestimmt werden—zumindest für Blasen im experimentell untersuchten Bereich. Dieser Bereich wurde soweit wie möglich ausgedehnt und entspricht im allgemeinen dem des Blasensiedens bei Umgebungsdruck oder darunter. Für Sättigungssieden (d.h. $T_{bulk} = T_{sat}$) ergibt sich als besonders einfaches und allgemeines Resultat eine Beziehung zwischen Abreißzeit und -durchmesser (oder -volumen). Diese Beziehung ist unabhängig von der Wachstumsgeschwindigkeit und der Dicke der thermischen Grenzschicht und lautet

$$\frac{D_D}{t_D^{2/3}} \simeq 1.5\left(\frac{\sigma}{\rho}\right)^{1/3} \quad \text{oder} \quad \frac{V_D}{t_D^2} \simeq 2.0\frac{\sigma}{\rho}.$$

Da sich für normale Flüssigkeiten σ/ρ nicht sehr stark ändert, ist diese Beziehung nur wenig von der Art der Flüssigkeit abhängig.

Die bekannte Erscheinung von 'gegen die Schwerkraft ablösenden' Blasen (d.h. in negativer Schwerkraft, wie an einer abwärts gerichteten Oberfläche) kann nun zum erstenmal unter kontrollierten Bedingungen beobachtet werden. Die Bedingungen, die ein solches Verhalten begünstigen, wurden bestimmt. Es sind dies besonders eine dünne thermische Grenzschicht und starke Unterkühlung. Eine unerwartete Festellung ist, daß positive Schwerkraft (Auftrieb) in manchen Fällen dazu führt, daß die Blase mit größeren Abmessungen ablöst als bei Schwerelosigkeit.

ДИФФУЗИОННЫЙ РОСТ ПУЗЫРЬКОВ ПАРА НА СТЕНКЕ ПРИ ЗАДАННОМ ГРАДИЕНТЕ ТЕМПЕРАТУР

Аннотация — Проведенные ранее исследования роста одиночных паровых пузырьков на стенке в направлении первоначально неподвижной жидкости распространены на ситуацию, когда в жидкости имеется заданная начальная температурная неоднородность. На основании анализа размерностей рассмотрены самые простые случаи (отсутствие силы тяжести, объем жидкости при температуре насыщения) и дано сравнение с ранее проведенными экспериментами и с результатами анализа задачи в еще более простой постановке, т. е. с первоначально постоянной температурой. Как и предполагалось, происходит чередование различных режимов, которые могут быть описаны количественно. При отсутствии гравитации можно было определить время отрыва пузырьков и их диаметр, по крайней мере, в пределах условий эксперимента. Экспериментальные условия в основном соответствовали пузырьковому кипению при атмосферном давлении или давлении ниже атмосферного. Кипение с насыщением (т. е. $T_{\text{об}} - T_{\text{нас}}$) описывается следующей очень простой и универсальной зависимостью между временем и диаметром (или объемом) отрыва, которая не зависит ни от скорости роста пузырьков, ни от толщины температурного пограничного слоя:

$$\frac{D_D}{t_D^{2/3}} \simeq 1{,}5\left(\frac{\sigma}{\rho}\right)^{1/3} \quad \text{или} \quad \frac{V_D}{t_D^2} \simeq 2{,}0\frac{\sigma}{\rho}.$$

Поскольку для обычных жидкостей отношение σ/ρ почти постоянно, то можно заключить, что приведенное выше соотношение справедливо для любого вида жидкости.

В рассматриваемых условиях впервые наблюдалось хорошо исследованное явление отрыва пузырьков в сторону, противоположную действию силы тяжести (т. е. при отсутствии выталкивающей силы, как например, в случае кипения на поверхности нагреваемой сверху пластины). Выяснено, что такое поведение обуславливается в основном тонким тепловым пограничным слоем и сильным недогревом. Неожиданный результат состоит в том, что в некоторых случаях при положительной силе тяжести (плавучесть) может происходить отрыв пузырьков большего диаметра, чем при ее отсутствии.